

Published in final edited form as:

Langmuir. 1995 April ; 11(4): 1368–1374. doi:10.1021/la00004a051.

Effects of Discrete Protein–Surface Interactions in Scanning Force Microscopy Adhesion Force Measurements

Joan K. Stuart and Vladimir Hlady*

Department of Bioengineering, University of Utah, Salt Lake City, Utah 84112

Abstract

The potential for measuring specific molecular recognition forces between probe-bound ligands and surface-bound proteins using a scanning force microscope (SFM) has recently gained much attention. Generally, observed discontinuities in the SFM force-displacement curves are attributed to the breaking of discrete, specific affinity bonds. The present study on the molecular recognition system composed of surface-immobilized anti-fluorescein IgG molecules and SFM probe-bound fluorescein ligands has demonstrated that similar intermittent discontinuities in the SFM force-displacement curves may in fact be largely due to nonspecific discrete interactions between the protein and the SFM probe. The mechanical behavior of the cantilever–spherical bead system used in this study is discussed, as it appears to cause a false indication of the separation distance between the surface and probe. The strong lateral interactions which result in “stick and slip”-like discontinuities seen in the adhesion curves are likely the result of localized adhesion due to the heterogeneous nature of proteins and the lack of molecular mobility allowed in the experimental system. The effect is magnified with increasing contact time between the protein and probe. Factors which may cause such anomalous behavior in a specific ligand–protein system are discussed in order to avoid misinterpretation of SFM adhesion measurements.

I. Introduction

The use of immobilized ligand–receptor interactions in biotechnology is quite common.¹ While many macroscopic techniques can determine the average amount, functionality, and macroscopic spatial arrangement of immobilized proteins, the true distribution and function of receptors on the submicron scale remain largely unknown. With the advent of new scanning probe microscopies, immobilized proteins and surface macromolecules have been re-examined on smaller and smaller scales. One instrument which has been widely used to image surface-bound molecules is the scanning force microscope (SFM).^{2,3} The SFM can provide nanoscale resolution of the topographical and other physical properties of a surface.⁴ Recently, it has been shown that a chemically modified SFM cantilever stylus could interact in a specific way with molecules on the specimen surface.⁵ When the specificity of interactions results in a force contrast, one can separate topographical and chemical surface information. In biological systems, where the molecular recognition events determine the specificity of interactions, the force contrast could be used to identify and map the

distribution of those surface-immobilized proteins which are capable of binding SFM stylus-bound ligands. The potential use of this concept in SFM measurements has been recognized recently by several research groups including ours.⁶⁻⁹

Here we describe SFM measurements of the interactions between surface-immobilized proteins and an SFM probe chemically modified with the protein-specific ligand. A model ligand-protein pair, fluorescein-antifluorescyl IgG, has been used for this purpose, as it is convenient to characterize its interactions using macroscopic fluorescence techniques. SFM force-displacement measurements were performed to compare the behavior and magnitude of nonspecific vs specific adhesion interactions. Upon initial inspection of the SFM adhesion curves, it appeared that specific and discrete unbinding events were taking place in both the specific and nonspecific systems. It became clear that relatively large nonspecific interactions between the probe and surface-bound proteins might have played an important role in almost every measurement. The observed “stick and slip”-like discontinuities and the influence of contact time on protein-SFM probe interaction are discussed in light of the mechanical nature of the SFM cantilever-probe system and the nonspecific protein-surface interaction kinetics, as are possibilities for minimizing these nonspecific effects in order to enhance the measurement of specific molecular recognition forces.

II. Materials and Methods

The experimental system consisted of a polished silicon wafer (roughness ~1 nm), onto which the protein, anti-fluorescyl IgG (monoclonal 9-40), was immobilized, and a commercial Si₃N₄ cantilever with no integral tip (thickness 0.3 μm, Park Scientific Inst., Mountain View, CA), onto which was glued a silica bead (15-25 μm diameter, Duke Scientific, Palo Alto, CA) derivatized with fluorescein. The immobilization chemistry was the same for both surfaces, and was covalent to assure that the ligand-protein pairs separate at the affinity binding site and do not desorb from the surface during the course of the experiments. The silicon wafer surfaces were first thoroughly cleaned and then oxidized using oxygen plasma (200 μm Hg, 50 W, 2 mid. The silicon wafer and silica bead surfaces were modified with 3-(glycidoxy)propyldimethylethoxysilane (GPS) (Hüls/United Chemical Technology, Bristol, PA), which leaves an epoxide group to be reacted with amine groups in both the IgG and fluorescein reagent 5-(((2-carbohydrazino)methyl)thio)acetyl)aminofluorescein, (Molecular Probes, Inc., Eugene, OR).^{10,11} The cantilevers were oxygen plasma cleaned for 25 s. The fluorescein-derivatized silica beads were glued (Speedbonder 325 Structural Adhesive, Loctite Corp., Newbury, CT) to the cantilever tip area using a micromanipulator. Figure 1a shows the fluorescence image of the fluorescein-coated bead glued onto the SFM cantilever.

The modified surfaces were characterized using several methods. An ESCA surface analysis¹² was performed after each surface modification step to confirm the presence of proteins and of fluorescein on their respective surfaces (data not shown here). Radiolabeling the protein with ¹²⁵I before immobilization was used to quantify the average surface coverage.¹³ The fluorescein titration of the specific anti-fluorescyl IgG silica surfaces was carried out using total internal reflection fluorescence (TIRF) spectroscopy¹⁴ in order to establish the functionality and the binding affinity of the immobilized anti-fluorescyl IgG.

Binding studies of the solution anti-fluorescyl IgG to the silica surface-immobilized fluorescein were also carried out using the TIRF technique.

To record the SFM adhesion curves, a custom-built external driver and detector system⁶ was combined with the NanoScope II (Digital Instruments, Inc., Santa Barbara, CA) SFM. The system enabled us to control the shape of the piezoelectric sample stage driving signal and the contact time between the probe and the sample surface. Figure 1b shows the displacement of the sample stage in the adhesion experiments. It was driven a distance of 1090 nm up and down (or vice versa, as indicated) for a specified period of time. Two types of adhesion measurements were performed: in the first, the piezo with the sample surface was brought into contact with the cantilever-glued bead (or stylus) using the stepper motor, and the piezo was then displaced away from the contact position and brought back (curve A, Figure 1b). In the second type of adhesion measurement, the piezo displacement was inverted. The bead and the sample surface, initially separated, were brought into contact and then pulled apart (curves B–D, Figure 1b). The period was either 2 or 8 s per half-cycle. In scheme D of Figure 1b, the bead and sample were brought into contact and remained in contact for 8 s before being withdrawn. In all cases, the detector signal was converted into force from the withdrawing part of the adhesion curve in contact using the manufacturer-provided spring constants, k , and the calibrated sample stage displacement, z , using $F = kz$.

The SFM adhesion curves were recorded for various sample surface–SFM probe combinations. Specific adhesion forces were measured between the fluorescein-derivatized SFM probe and the specific surface-immobilized anti-fluorescyl IgG. These measurements were performed using various piezo displacements in order to study mechanical and kinetic effects. As negative control experiments, the adhesion interactions between a fluoresceinated silica bead and a GPS-derivatized surface (with no protein) and between a fluoresceinated silica bead and a nonspecific, surface-immobilized anti-HSA IgG were measured. In additional control experiments, the adhesion interactions between a clean, underivatized integral SFM stylus (100 μm long triangular cantilever, $k = 0.37 \text{ N/m}$) and surface-immobilized anti-fluorescyl IgG were also recorded. All adhesion measurements were performed in 10 mM phosphate buffer at pH 7.7.

The mechanical properties of the bead–cantilever system were modeled using a finite element analysis (FEA) program.¹⁵ The FEA cantilever model was made up of 20 elements, and the spherical bead was modeled as firmly attached over an area close to that of glued bead. The cantilever, positioned at 12° from horizontal, was subjected to various loads in the normal and tangential directions. The nodal displacements were recorded and the resulting angular deflections were calculated.

III. Results

Immobilization of ^{125}I -labeled anti-fluorescyl IgG showed that the protein surface density, Γ , was $0.5 \mu\text{g}/\text{cm}^2$, an amount close to that of an IgG monolayer.¹⁶ The SFM topographic imaging supported these results (data not shown here). The TIRF fluorescein titration of the anti-fluorescyl IgG silica surface showed that the binding affinity of the immobilized anti-fluorescyl IgG is $2 \cdot 10^{-7} \text{ M}^{-1}$, compared with nominal solution affinity of $3.3 \cdot 10^{-7} \text{ M}^{-1}$ (J.

Herron, personal communication). Binding of the solution anti-fluorescein IgG to the surface-immobilized fluorescein resulted in a 70% quenching of fluorescence, indicating thus that the anti-fluorescein IgG binding to the immobilized fluorescein indeed took place.

Figure 2 shows typical results from a series of SFM adhesion measurements taken using the molecularly specific system, i.e. a fluoresceinated SFM probe and anti-fluorescein IgG surface. The first measurement was performed within 2 s of initial contact between the probe and surface (Figure 2, curve a). The adhesion force was relatively small, 0.2 nN, as was the apparent probe–IgG surface separation (50 nm) at the jump out of contact. The second measurement (Figure 2, curve b) was taken after 1 min of contact. Note that not only has the adhesion force increased, but there were discrete jumps that occur along a separation distance of 250 nm before the jump out of contact. The jagged behavior of the adhesion force curve was repeated to an even greater extent in the third measurement of the series (Figure 2, curve c), before which the probe and sample rested in contact for 2 min. When the probe was positioned on a new area of the anti-fluorescein IgG surface the main features of the curves a–c were repeatedly observed. The “stick and slip”-like discontinuities¹⁷ were seen throughout several sets of measurements whenever the contact time was longer than a few seconds.

The adhesion forces were measured under otherwise identical conditions for the two control systems (Figure 3). Curve a was measured for the interactions between a fluoresceinated probe and a nonspecific, anti-HSA IgG surface. Curve b was measured for the adhesion between a clean, nonderivatized commercial Si₃N₄ tip and the anti-fluorescein IgG. In both cases, the discontinuous nature of the probe–sample separation was evident. Figure 4 shows a typical SFM adhesion curve for the negative control experiment, where the GPS-derivatized silicon surface adhered to the fluoresceinated SFM bead with no protein present in between. The adhesive force was large (7 nN), and the curve showed no intermittent discontinuities. The apparent separation was zero for a large part of the adhesion curve only to increase smoothly to 200 nm prior to the jump out of contact.

Figures 2–4 have all been recorded using the contact–withdrawal–contact displacement of the sample stage (scheme A, Figure 1b). In Figure 5, the interactions of the specific system were measured with an inverted displacement of the sample stage, so that the sample approached the probe and then withdrew, thus allowing no extra time for equilibration before the actual adhesion measurement. The first measurement (Figure 5, curve a) was taken with a 2 s half-cycle. The magnitude of the force was relatively small, 0.2 nN, and the jump out of contact was preceded by the rounded part of the adhesion curve. After several 2 s half-cycle measurements, the 8 s half-cycle displacement scheme was used to drive the sample stage (scheme C, Figure 1b). During this measurement the probe and the IgG surface spent approximately 4 times longer time in contact than in the 2 s half-cycle measurement. With a longer time in contact, the magnitude of the adhesion significantly increased and the “stick and slip”-like discontinuities appeared (Figure 5, curve b). The jagged behavior of the adhesion curve occurred not only when the cantilever was in the negative load regime, i.e. below its resting position, but also when it was exerting positive load onto the surface. In addition to that, a small apparent separation showed between the probe and the surface in the region of positive load, i.e. above the resting position of the cantilever.

In order to further clarify the behavior of the cantilever–bead system in contact with the specific IgG surface, the adhesion curves were measured using the sample stage displacement scheme during which the sample moved 1090 nm upward in 2 s, rested in this position for 8 s, and then moved 1090 nm downwards in 2 s (curve D, Figure 1b). The typical result is shown in Figure 6, where the cantilever deflection is plotted in force units vs the displacement time. The upper panel shows a magnified view of the cantilever angle change while in contact. It can be seen that during the contact period the cantilever angle slowly changes due to rolling of the probe into a more relaxed position. The final part of the adhesive curve (time > 10 s) showed several discontinuous jumps out of contact.

IV. Discussion

In this study we have investigated specific ligand–protein and nonspecific interfacial protein interactions using SFM adhesion experiments in which the adhesive forces between the SFM probe and the protein-coated surfaces are determined from the cantilever deflection during their separation. The experimental results indicated that the magnitude of the adhesion was determined by the time of the contact between the probe and the surface: the weak adhesion forces, measured after very short contact times, increased in magnitude following an extended contact. The SFM adhesion curves also displayed a discontinuous “stick and slip”-like shape (Figures 2–5). The suggestion that the discrete steps reflect unique unbinding events between a single ligand–protein pair or a population of the pairs has been forwarded by several research groups^{7–9} including us.⁶ In this scenario, as the cantilever with the probe-immobilized ligands is separated from contact with the sample-immobilized proteins, tension is created between a certain population of ligand–protein pairs until the bonds are broken. As a result, the cantilever performs a small jump upward, generating tension at another population of specific bonds that were not challenged before. Hence, it was concluded that the force of a single discrete unbinding event could be measured. The above scenario could indeed happen in the case of soft protein substrates, such as those employed by Florin et al.⁷ In the present study, however, both the protein-carrying substrate and the SFM probe were relatively rigid solids, Si/SiO₂ and silica, respectively. According to the results from the present study, the final jumps of the cantilever into its resting position occurred *after* the SFM probe with ligands and the proteins at the sample surface were apparently separated by more than hundreds of nanometers (Figure 2 and 5). This general feature could neither be explained by a deformation of SiO₂ nor by a “stretching” of surface immobilized proteins. The immobilization of IgG was carried out using 3-carbon atom spacers, and while any local multilayer protein formation could not be entirely ruled out, the average protein surface coverage indicated a monolayer coverage. Alternate effects needed to be considered to explain this separation distance anomaly.

Since the control experiments (Figure 3) also showed a discontinuous nature of the SFM adhesion curve, it was concluded that the intermittent discontinuities are more related to general interfacial protein interactions than to the specific ligand–protein unbinding events. The absence of the discrete steps in the negative control experiments when no protein was present in the system (Figure 4), led us to the conclusion that lateral forces are responsible for apparent large probe–surface separation distances, while in the protein-containing

systems, the discontinuous shape of the adhesion curves were primarily due to the discrete protein–SFM probe interactions. The discrete protein–SFM probe interactions might have originated from both specific and nonspecific unbinding events. We hypothesize that the interplay among (1) the experimental geometry of the SFM, cantilever–bead system, (2) the multiplicity and the discreteness of the protein–SFM probe interactions, and (3) kinetically determined magnitudes of the related adhesion force was responsible for the large apparent separation distances and the discontinuous “stick and slip”-like shape of the adhesion curves. We further discuss each of these three factors below.

Effect of Geometry of the SFM Cantilever–Bead System

We first consider the mechanical behavior of the SFM cantilever–bead system. Figure 7a shows an ideal case: oriented at a 12° angle from horizontal, the cantilever only *bends* during the sample displacement. As the sample is withdrawn, if the probe remains in contact due to adhesion, it will also have to translate horizontally in the x -direction by a distance approximately equal to 21% of the vertical displacement. As a typical sample displacement in our study was $1\ \mu\text{m}$, the horizontal translation of the probe could be as much as $210\ \text{nm}$, a distance over which lateral forces will affect the cantilever response.

The ideal case of cantilever bending occurs only in the absence of lateral forces.^{18,19} The major effect of lateral forces acting during the horizontal translation of the SFM probe over the surface is the *buckling* of the cantilever. Since the cantilever is at 12° angle, as the sample is displaced upward and contacts the SFM probe, lateral forces will cause the probe to roll forward and the cantilever to buckle (Figure 7b). When the sample in contact with the SFM probe is withdrawn downward beyond the cantilever resting position, the probe will roll backward and the cantilever will buckle in the opposite fashion. Any rolling of the probe and buckling of the cantilever will change the cantilever angle and result in a false separation reading. The cantilever angle change caused by buckling is strongly affected by the large size of the SFM probe. In the optical lever detection system used in this study, an external linear position sensitive detector positioned at ca. $10\ \text{cm}$ away from the cantilever made the detection system very sensitive to small changes of the cantilever angle.⁶

According to Warmack et al.,¹⁹ lateral forces will cause angle changes that are quite small compared with angle changes due to the normal forces, but the effect will increase for very thin cantilevers and large SFM probes. The latter two conditions were always met in the present study. The result of the negative control experiment (Figure 4) could be explained by the effect of buckling of the cantilever. Using the formalism developed by Warmack et al.¹⁹ and assuming that no lateral forces existed between the SFM spherical probe and the GPS-derivatized surface prior to the jump-out of contact, i.e. up to the $520\ \text{nm}$ displacement, one can calculate that the angle of the cantilever just prior to the jump-out should be -0.48° different from its resting position angle ($100\ \mu\text{m}$ -long, $0.3\ \mu\text{m}$ thick rectangular cantilever with a $20\ \mu\text{m}$ diameter bead and the sensing laser spot $80\ \mu\text{m}$ away from the cantilever base). In Figure 4, one can find that the apparent separation at the jump-out was $200\ \text{nm}$. The cantilever angle that would cause such a separation, i.e. the $520\ \text{nm}$ displacement minus the apparent $200\ \text{nm}$ separation, is -0.34° different from the resting position angle, rather

than -0.48° . The $+0.14^\circ$ difference between the two angles is presumably due to the lateral probe–surface interactions that caused the cantilever buckling.

We have simulated the behavior of our cantilever–probe system using an FEA program in order to estimate the upper limit of cantilever angle changes due to buckling. Figure 7c shows the geometry of the FEA model. Loading the cantilever with vertical and lateral forces, in the cases where the probe was free to move in any direction, caused a smoothly increasing bending of the cantilever. In order to simulate the combined effect of vertical displacement and the very strong local adhesion of the probe, the probe was fixed in the x -direction and allowed to displace only vertically. As a result the cantilever buckled. Angle changes for the buckled cantilever contained both positive and negative angle changes distributed along the cantilever (Figure 7d). This effect of angle change will propagate as an error in both the separation distance calculations and in the adhesion force evaluation. It is clear that judicious positioning of the optical lever laser focus is a necessary prerequisite for reproducible adhesion experiments. In some cases the laser might be focused right onto the region of the cantilever where the temporary angle changes are close to zero; as a consequence the experimental results may suggest that the cantilever is in its resting position although, in fact, it might have been significantly displaced and buckled!

Effect of Discreteness of Strong Protein–SFM Probe Interactions

The fixing of the SFM probe in the x -direction during the FEA simulations implied that inflections will occur only when the magnitude of actual lateral forces is larger than the strain energy stored in a buckled cantilever. Consider the case of the cantilever which, during the vertical displacement of the sample, laterally translates along the surface with a given (small) friction and then encounters an area of very strong adhesion. The FEA results indicated that the discrete areas of very strong adhesion will cause an additional, temporary buckling of the cantilever up to the point where the adhesion energy equals the strain energy of a buckled cantilever. The additional buckling will result in an angle change that will, depending on the position of the laser focus, cause a false reading of separation and total adhesion force. As the probe ends its sliding over the very strong adhesion area, or as the cantilever stored energy exceeds the local adhesion energy, the cantilever, still in contact with the surface, will tend to relax into a less buckled position. This relaxation process may appear as a small jump out of contact, except that it will not bring the cantilever to its resting position but to some apparent intermediate separation dictated by the position of the optical lever laser focus and by the balance between remaining vertical and lateral contact forces between the probe and the surface.

It is possible that in our experiments (Figures 2, 5, and 6) the areas of strong adhesion had a specific ligand–protein component. However, the control experiments (Figure 3) indicated that the same effects are observed with the nonspecific proteins. In either case, discretely distributed strong adhesion areas sampled by the SFM bead during its lateral translation over the surface are assumed to be responsible for the observed “stick and slip”-like discontinuities in the SFM adhesion curves.

Effect of the Protein–Probe Interaction Kinetics

It is hypothetically possible that the kinetic laws for specific binding of ligand into the protein binding site and for nonspecific surface adsorption of protein are sufficiently different to allow for the discrimination between the two processes on the basis of contact time. It is well-known that the rate of nonspecific protein adsorption onto solid/liquid interfaces can be limited by the actual rate of protein attachment to the surface.²⁰ We observed that in the SFM adhesion experiments the magnitude of adhesion was determined by the contact time between the probe and the protein-coated surface. However, adhesion after a prolonged contact time could not be abolished with an excess of free ligand in solution. The effect of the free ligand excess on short contact time adhesion was difficult to evaluate experimentally.

Another possible approach to predicting the outcome of the interplay between specific and nonspecific interaction events is to consider the difference between the lifetimes of specific molecular recognition and nonspecific adsorption bonds. Specific bonds of moderately high affinity are predicted to break under 100 pN of applied force per bond when assisted with thermal dissociation of bonds in equilibrium and under 400 pN force per bond when the tension across the bond is developed instantaneously.²¹ While the predicted separation forces are additive for any number of bonds in equilibrium, the forces applied to break the fixed bonds, i.e. bonds which cannot re-form, will regulate the bonds' collective lifetime. The lifetime of fixed multiple bonds exponentially increases with the number of bonds and decreases with the applied force.²¹ Extrapolation of these predictions to our experiments indicates that the multiple fixed bonds of nonspecific protein adsorption will resist longer before breaking apart due to a higher tension. It is not surprising that the nonspecific protein adsorption is often considered to be irreversible.²⁰

Using the chord theorem²² one can estimate that a 20 μm diameter bead and proteins on a flat surface interact over a contact area of 0.6 μm^2 , with a circumference of 2800 nm. If IgG molecules along this circumference all form bonds with ligands, there will be more than 400 specific bonds formed. If challenged simultaneously, these bonds could resist a force of 160 nN. In reality, the bonds will thermally dissociate and the actual sequence of the bonds breaking will be influenced by the rolling behavior of the SFM bead. Accordingly, the separation forces are expected to be much smaller. In addition to the circumference IgG, there will be IgG molecules distributed in the whole contact area, approximately 14 000 in number. When the contact is formed, not all of them will be able to react with ligands due to the restriction of lateral diffusion, but could react with the probe interface in a nonspecific way. Since the area/circumference molecular ratio is quite large, if only a small part of the proteins inside the circumference are participating in nonspecific adsorption, their adhesion will dominate.

In this physical picture of protein–probe interactions, the longer the probe is in contact with the sample, the more the proteins will be able to bind, rearrange, and bridge nonspecifically to the SFM probe. The picture is consistent with the kinetic effects we have observed, in which the magnitude and discontinuous nature of the adhesion force profiles increases with contact time. How, then, could one minimize these deleterious nonspecific interactions? In biology one finds that there is a very strong and long-ranged repulsive potential between the

biological surfaces and that cells are not generally adhesive to each other. The physical origin of this potential is the polysaccharide layer on the exterior surface of the cell membrane, the glycocalix. Upon the cell contact with a surface, the polysaccharide chains are compressed and lose conformational entropy, water molecules are removed from the hydrophilic sugar residues thereby increasing the chemical potential of the solvent, and upon further compression, an elastic response is elicited from the polysaccharide chains. The resulting repulsive potential acts as a spatial barrier for the nonspecific interactions that are so ubiquitous in the vicinity of solid surfaces. The mimetic system we are currently exploring emulates that effect by using long chain polyethylene oxide spacers between the substrate and the protein and between the probe and ligands. It has been shown in previous SFM studies that these grafted chains will elicit steric repulsion upon compression²³ and will practically eliminate nonspecific protein adsorption.²⁴

V. Conclusions

In measuring protein interactions with the SFM, it was noted that the adhesion curves reflect a greatly exaggerated separation distance and a discontinuous “stick and slip”-like behavior. The mechanical nature of the experimental system, that of a spherical bead glued to the cantilever, is found to magnify these anomalous effects. If the probe remains in contact with the sample while it is being withdrawn, relatively large discrete lateral forces can cause rolling and buckling of the cantilever, leading to a false indication of separation distance. These forces are probably caused by very strong areas of localized adhesion due to protein–probe interactions. These interactions cause buckling and unbuckling of the cantilever as the probe is translated over a microheterogeneous sample, the phenomenon which appears in the adhesion curves as discrete unbinding events or “stick and slip”-like jumps. The magnitude and discontinuous nature of the adhesion curves increased with sample contact time. The longer the probe is in contact with the sample, the more the proteins will be able to bind, rearrange, and bridge with the probe. Hence, the effects of nonspecific protein–probe interactions can be quite large and may even dominate any specific effects. It is necessary to eliminate or control nonspecific protein interactions, by creating surfaces with a repulsive, protein–adsorption resistant nature. On the other hand, nonspecific protein–probe interactions measured with SFM can become an additional technique for developing a better understanding of the general nature of protein interfacial interactions.

Acknowledgments

This work was supported by research grants from the Whitaker Foundation and the NIH (R01-HL44538). The authors gratefully acknowledge discussions with M. Pierce, J. D. Andrade, H. P. Jennissen, and M. Radmacher and wish to thank J. Herron, H.-K. Wang, and A.-P. Wei for providing the IgG and assistance with its characterization, and A. Pungor and P. Dryden for their technical expertise with the instrumentation.

References

- (1). Hermanson, GT.; Mallia, AK.; Smith, PK. Immobilizedmunity Ligand Techniques. Academic Press; San Diego, CA: 1992.
- (2). Hansma HG, Hoh JH. Biological Imaging with the Atomic Force Microscope. Annu. Rev. Biophys. Biomol. Struct. 1994; 23:115–139. [PubMed: 7919779]

- (3). Engel A. Biological Applications of Scanning Probe Microscopes. *Annu. Rev. Biophys. Biophys. Chem.* 1991; 20:79–108. [PubMed: 1867727]
- (4). Sarid, D. Scanning Force Microscopy: with Applications to Electric, Magnetic and Atomic Forces. Lapp, HSM., editor. Vol. Vol. 2. Oxford University Press; New York: 1991. Oxford Series on Optical Sciences
- (5). Frisbie CD, Rozsnyai LF, Noy A, Wrighton MS, Lieber CM. Functional Group Imaging by Chemical Force Microscopy. *Science*. 1994; 265:2071–2074. [PubMed: 17811409]
- (6). Pierce M, Stuart JK, Pungor A, Dryden P, Hlady V. Adhesion Force Measurements Using an Atomic Force Microscope Upgraded with a Linear Position Sensitive Detector. *Langmuir*. 1994; 10:3217–3221.
- (7). Florin E-L, Moy VT, Gaub HE. Adhesion Forces Between Individual Ligand-Receptor Pairs. *Science*. 1994; 264:415–417. [PubMed: 8153628]
- (8). Lee GU, Kidwell DA, Colton RJ. Sensing Discrete Streptavidin-Biotin Interactions with Atomic Force Microscopy. *Langmuir*. 1994; 10:354–357.
- (9). Moy VT, Florin E-L, Gaub HE. Intermolecular Forces and Energies Between Ligands and Receptors. *Science*. 1994; 266:257–259. [PubMed: 7939660]
- (10). Sanders, A. Diplomarbeit, Modifizierung von Kieselgel- und Quarzglasoberflächen zur Proteinadsorption. Universität-Gesamthochschule Essen; 1994.
- (11). Sundberg L, Porath J. Preparation of Adsorbents for Biospecific Affinity Chromatography I. Attachment of Group-Containing Ligands to Insoluble Polymers by Means of Bifunctional Oxiranes. *J. Chromatogr.* 1974; 90:87–98. [PubMed: 4824665]
- (12). Andrade, JD. X-Ray Photoelectron Spectroscopy In Surface and Interfacial Aspects of Biomedical Polymers. In: Andrade, JD., editor. *Surface Chemistry and Physics*. Vol. Volume 1. Plenum Press; New York: 1985. p. 105-196.
- (13). Lin J-N, Andrade JD, Chang I-N. The Influence of Adsorption of Native and Modified Antibodies on Their Activity. *J. Immunol. Methods*. 1989; 125:67. [PubMed: 2558139]
- (14). Hlady, V.; Van Wagenen, RA.; Andrade, JD. Total Internal Reflection Intrinsic Fluorescence (TIRIF) Spectroscopy Applied to Protein Adsorption In Surface and Interfacial Aspects of Biomedical Polymers. In: Andrade, JD., editor. *Protein Adsorption*. Vol. Volume 2. Plenum Press; New York: 1985. p. 81-119.
- (15). Nairn, J. JANFEA 11. Salt Lake City, UT: 1994.
- (16). Grabbe ES. Total Internal Reflection Fluorescence with Energy Transfer: A Method for Analyzing IgG Adsorption on Nylon Thin Films. *Langmuir*. 1993; 9:1574–1581.
- (17). Gee ML, McGuiggan PM, Israelachvili JN, Homola AM. Liquid to Solidlike Transitions of Molecularly Thin Films under Shear. *J. Chem. Phys.* 1990; 93:1895–1906.
- (18). Hoh JH, Engel A. Friction Effects on Force Measurements with an Atomic Force Microscope. *Langmuir*. 1993; 9:3310–3312.
- (19). Warmack RJ, Zheng X-Y, Thundat T, Allison DP. Friction Effects in the Deflection of Atomic Force Microscope Cantilevers. *Rev. Sei. Instruments*. 1994; 65(2):394–399.
- (20). Andrade JD, Hlady V. Protein Adsorption and Materials Biocompatibility: Tutorial Review and Suggested Hypotheses. *Adv. Polym. Sci.* 1986; 79:1–63.
- (21). Baltz JM, Cone RA. The Strength of Non-covalent Biological Bonds and Adhesions by Multiple Independent Bonds. *J. Theor. Biol.* 1990; 142:163–178. [PubMed: 2352430]
- (22). Israelachvili, JN. *Intermolecular and Surface Forces*. 2nd ed.. Academic Press; San Diego, CA: 1992.
- (23). Lea AS, Andrade JD, Hlady V. Compression of Polyethyleneglycol Chains Grafted onto Silicon Nitride Surface as Measured by Scanning Force Microscopy. *Colloids Surf. A: Physicochem. Eng. Aspects*. 1994; 93:349–357.
- (24). Lin Y-S, Hlady V, Gölander C-G. The Surface Density Gradient of Grafted Polyethyleneglycol: Preparation, Characterization and Protein Adsorption. *Colloids Surf. B: Biointerfaces*. 1994; 3:49–62.

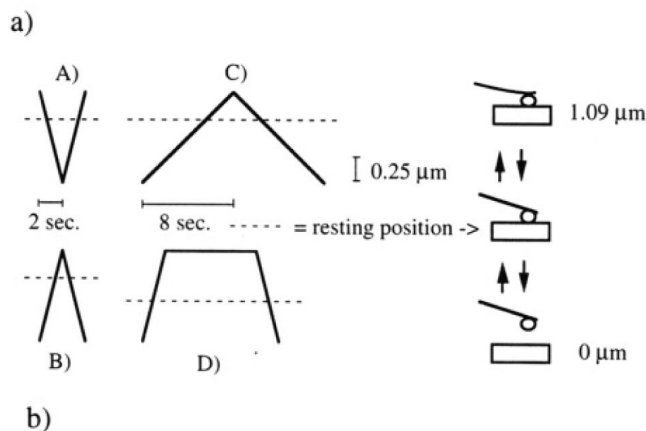


Figure 1. (a) Fluorescence image of a fluorescein-modified spherical silica bead, glued to the end of an SFM cantilever. (b) Shape of the input piezo signals driving the sample. The total vertical travel is 1090 nm, as shown on the right. In scheme A, the probe and sample are initially in contact, until the piezo sample is activated downward for a distance of 1090 nm over 2 s and then reapproaches the probe over the same period. In schemes B–D, the signal is inverted, so that the sample and probe are initially separated until the sample approaches and withdraws over either 2 or 8 s, as indicated. In scheme D, the sample approaches the probe over 2 s, remains in contact for 8 s, and then is withdrawn over 2 s.

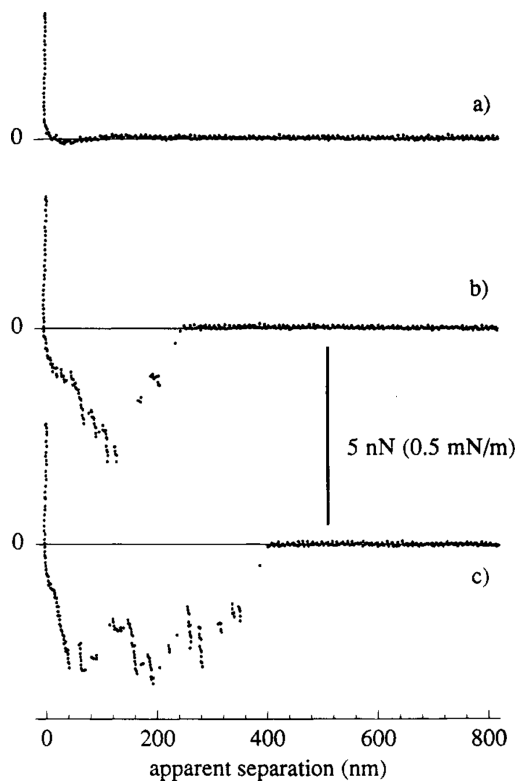


Figure 2.

Adhesion curves measuring the interactions of a molecularly specific system, i.e. between a fluorescein-modified probe and a silicon surface carrying immobilized anti-fluorescyl IgG. The piezo input signal is as in Figure 1b, scheme A, where the probe and sample are allowed to remain in contact/equilibrium for any length of time before measuring. Curve a measures the force (in parentheses, normalized force, *FIR*) versus apparent sample-probe separation for an equilibrium time of only 2 s. Curve b shows the adhesion after 1 min of contact, and curve c shows that after 2 min of contact.

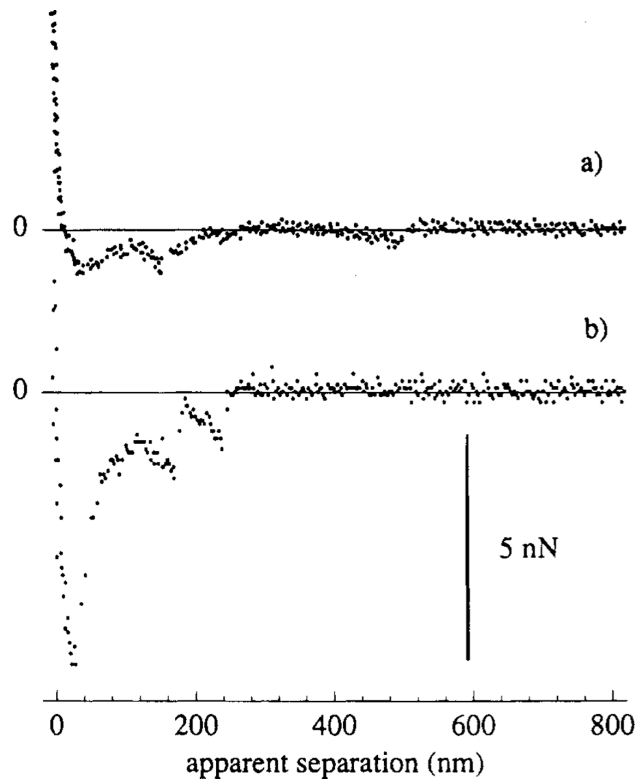


Figure 3. Two control measurements, taken using scheme A of Figure 1b. Curve a shows the adhesion interactions between a fluoresceinated spherical probe and a nonspecific immobilized anti-HSA IgG surface. Curve b shows the adhesion interactions between a clean, underivatized integral tip and a specific anti-fluorescyl IgG surface.

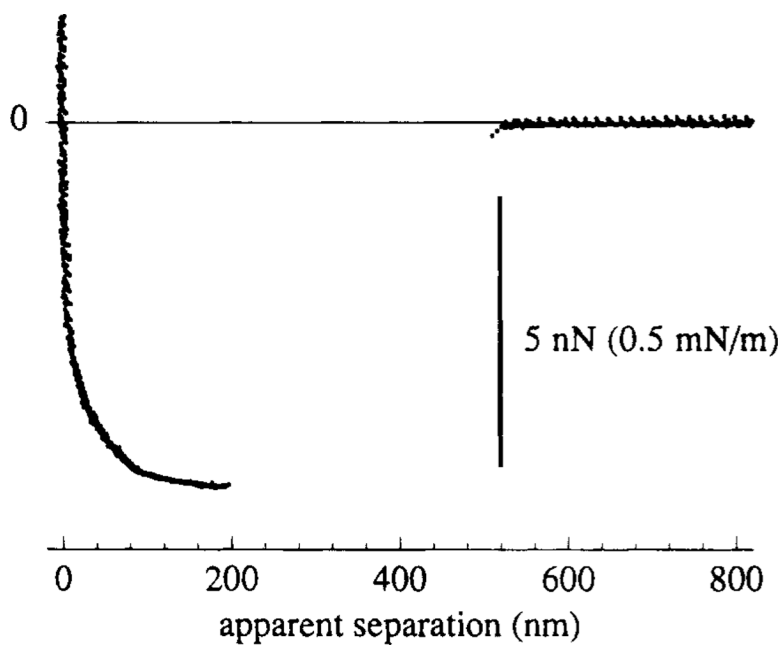


Figure 4. Negative control measurement, taken using scheme A of Figure 1b, showing the adhesion between a fluoresceinated probe and a surface covered with only the GPS spacer molecule.

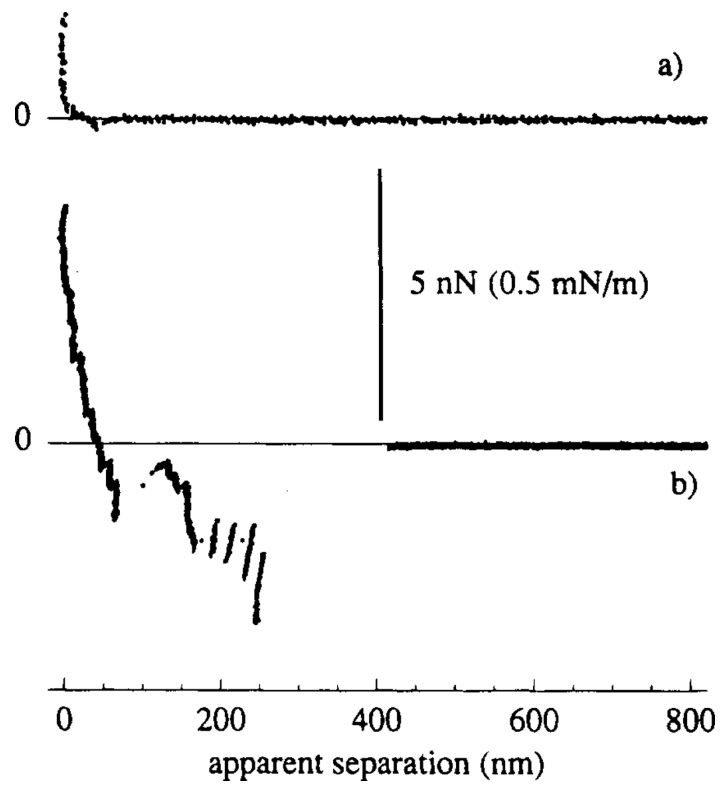


Figure 5. Specific adhesion measurements (using fluorescein and anti-fluorescyl IgG) taken with inverted sample driving signals, as in Figure 1b. Curve a is taken using scheme B (2 s half-cycle) and curve b is taken using scheme C (8 s half-cycle).

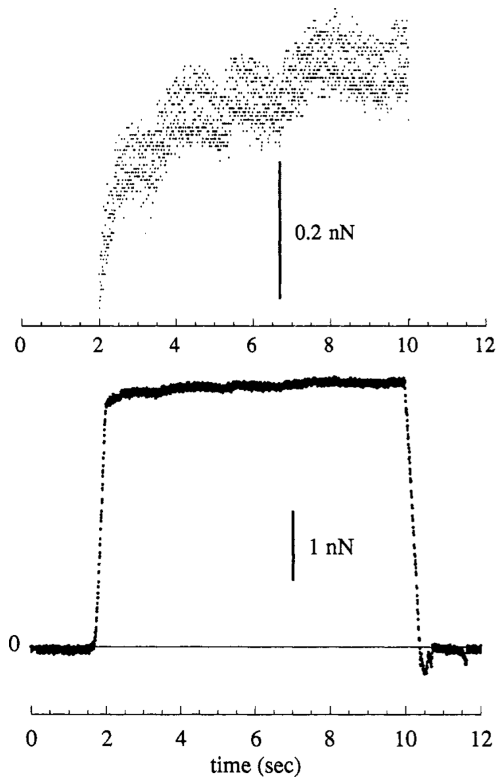


Figure 6. Adhesion curve, plotted as force vs time, obtained using scheme D of Figure 1b, where the sample approached the probe in 2 s, waited for 8 s, and then withdrew for 2 s. The upper panel shows a magnified view of the 8 s waiting period where the probe is shown to relax.

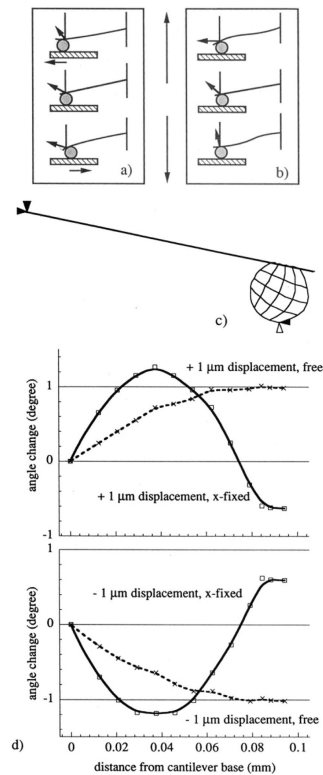


Figure 7.

Effect of lateral forces on cantilever mechanical behavior. Part a shows a cartoon of cantilever bending with sample displacement, as a result of its resting position at 12° . Part b depicts cantilever buckling, such as what would happen if the probe encountered a high-adhesion area, and the corresponding angle changes. Part c shows the finite element analysis model at its resting position, with nodal forces applied to the probe. In part d are the results of the finite element analysis. The upper panel shows the calculated angle change of the cantilever as a function of distance from the cantilever base, both for the situation where the probe was allowed to move freely in the horizontal direction while being displaced $1 \mu\text{m}$ in the upward direction and where the probe was fixed horizontally while being displaced $1 \mu\text{m}$ vertically. The lower panel shows the same results, calculated for displacements of $1 \mu\text{m}$ in the opposite downward direction.